

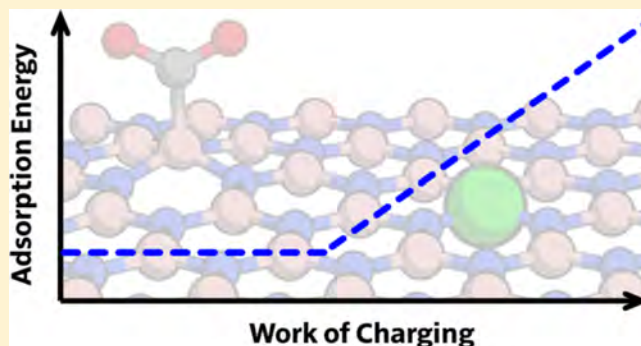
Overcoming Old Scaling Relations and Establishing New Correlations in Catalytic Surface Chemistry: Combined Effect of Charging and Doping

Kristof M. Bal*¹ and Erik C. Neyts¹

Department of Chemistry, Research Group PLASMANT, University of Antwerp, Universiteitsplein 1, 2610 Antwerp, Belgium

Supporting Information

ABSTRACT: Optimization of catalytic materials for a given application is greatly constrained by linear scaling relations. Recently, however, it has been demonstrated that it is possible to reversibly modulate the chemisorption of molecules on nanomaterials by charging (i.e., injection or removal of electrons) and hence reversibly and selectively modify catalytic activity beyond structure–activity correlations. The fundamental physical relation between the properties of the material, the charging process, and the chemisorption energy, however, remains unclear, and a systematic exploration and optimization of charge-switchable sorbent materials is not yet possible. Using hybrid DFT calculations of CO₂ chemisorption on hexagonal boron nitride nanosheets with several types of defects and dopants, we here reveal the existence of fundamental correlations between the electron affinity of a material and charge-induced chemisorption, show how defect engineering can be used to modulate the strength and efficiency of the adsorption process, and demonstrate that excess electrons stabilize many topological defects. We then show how these insights could be exploited in the development of new electrocatalytic materials and the synthesis of doped nanomaterials. Moreover, we demonstrate that calculated chemical properties of charged materials are highly sensitive to the employed computational methodology because of the self-interaction error, which underlines the theoretical challenge posed by such systems.



INTRODUCTION

The development and optimization of new high-performing heterogeneous catalysts and interfacial materials is an ongoing challenge. A major limitation of most conventional catalytic processes is the existence of linear scaling relations that connect the activity of many materials for a wide range of surface reactions.^{1–3} This means that although many chemical parameters of a material can in principle be independently changed, resulting surface properties—such as binding energies and reaction rates—are highly correlated. In practice, the chemical properties of most materials are only found in a very narrow range manifesting in a so-called “volcano plot” that characterizes many catalysts.^{2,3}

Overcoming these scaling laws is a major point of interest in catalysis research and poses an important challenge to theory and experiment alike. Using theoretical calculations, non-equilibrium reaction conditions have been proposed as a way to widen the parameter space of the catalytic process. On one hand, the electronic properties of a catalyst could be dynamically tuned through, for example, ferroelectric polarization⁴ or external electric fields,⁵ in order to access properties outside of standard volcano-type relations. On the other hand, the catalyst could be integrated into a nonequilibrium nonthermal plasma environment, in which nonequilibrium charge distributions⁶ or overpopulated vibrationally excited

molecular states⁷ can significantly alter the surface chemistry beyond what would be accessible at thermodynamic equilibrium. The remarkable success stories of these preliminary investigations hint at the existence of a completely new, unexplored, discipline in surface science.

A particularly interesting application of such nonequilibrium states to interfacial processes is the controlled charging or polarization of materials. It has been most commonly investigated for reversible gas adsorption in the context of CO₂ capture and H₂ storage,⁸ on 2D nanomaterials such as hexagonal boron nitride (h-BN), where strong electric fields⁹ and excess charges¹⁰ can be used as a “switch” to reversibly change the affinity of the material for a particular molecule. Depending on the electric state, a material can interact differently with molecules, and can hence have properties that are not solely determined by its chemical composition or confined by common linear scaling relations. Effectively, a single material could cycle through a set of different chemical properties, each of which is “just right” for a specific process step (e.g., gas capture and subsequent release). Furthermore, wider implications of charging for catalytic reactions,⁶ material

Received: February 6, 2019

Revised: February 20, 2019

Published: February 20, 2019

synthesis,¹¹ and phase transitions¹² have also been suggested. A whole new range of processes becomes available even for well-characterized materials, and many new exciting consequences of this phenomenon are awaiting discovery.

Because of the novelty of the research field, little systematic insight into the mechanisms underpinning charge-tuned gas adsorption has so far been gained. CO₂ capture has been most commonly investigated; electron injection can turn the molecule–surface interaction from physisorption into chemisorption for several 2D materials, primarily graphitic nitrides.^{8,10,13–16} In most systems, the chemisorption energy appears to be correlated to the overall electron density—higher densities induce stronger binding—but there is no obvious method to a priori predict on which material binding is strongly charge-responsive, what the required charge density for chemisorption is, or to what extent charge-responsive properties of a given material can be tuned or engineered. The fundamental physics behind charge-responsive adsorption remains unknown, which means that the specific materials and charging conditions reported in the literature seem somewhat arbitrary, although some efforts have recently been made to develop appropriate and consistent computational methodologies free of artefacts, opening the door for more systematic studies.¹⁷

One underexplored aspect of charge-modulated molecular adsorption has been its relation to the processes of charging itself. Indeed, if adsorption on a material becomes more exothermic upon negative (positive) charging, this additionally released energy must have been provided by the injection of excess electrons (holes); bringing a material to a nonzero net charge requires a certain amount of work, which in some cases can be recovered in the form of improved chemisorption. The precise balance between supplied charging energy and obtained heat of adsorption is an important aspect by which the suitability of candidate charge-controlled gas capture processes should be judged. Moreover, once this relation is understood, it becomes possible to systematically screen and optimize new materials, and specifically select or control the surface processes at catalytic materials for arbitrary charge states. Essentially, such knowledge would give charge-modulated process on surfaces an analogue to the scaling relations in traditional (thermo)catalysis, which provide a simple way to explore and characterize a multidimensional material space in terms of low-dimensional correlations, and simplify the search for catalysts with certain desired properties.^{1–3}

In this contribution, we show how charge-modulated adsorption on 2D nanomaterials is governed by simple fundamental correlations. Using CO₂ adsorption on h-BN as a paradigmatic test case, we demonstrate the existence of a linear one-to-one relation between work of charging and chemisorption strength, and reveal how introduction of defects can tune the efficiency and strength of charge modulation. We then discuss how these insights can lead to the systematic development of new materials for sorption and catalysis.

■ COMPUTATIONAL DETAILS

General Methodology. Density functional theory (DFT) calculations were carried out with CP2K^{18,19} in the GPW formalism²⁰ with GTH pseudopotentials.^{21,22} Dispersion corrections were omitted in order to purely capture electronic contributions to the energy. To minimize basis set incompleteness errors, the Kohn–Sham orbitals were

expanded in a large doubly polarized triple- ζ (m-TZV2P) basis set,²³ while the cutoff for the density was 1000 Ry. Computation of exact exchange was made feasible by the auxiliary density matrix method,²⁴ employing a small uncontracted polarized triple- ζ (pFIT3) basis. We used PBE²⁵ as semilocal exchange–correlation functional, whereas hybrid calculations were carried out with HSE06.^{26,27}

The predicted band gap by HSE-type functionals is dependent on the effect range of the exact exchange term, which is controlled by a screening parameter ω , and defined by the limiting cases of $\omega = 0$ (exact exchange over the full interaction range, i.e., the PBE0 functional) and $\omega \rightarrow \infty$ (no exact exchange, or standard fully semilocal PBE). A value of $\omega = 0.11$ a.u. is most commonly recommended and used in the standard HSE06 functional, together with a theoretically justified²⁸ 0.25 fraction of exact exchange.²⁷ HSE06 is untested for this type of charge-modulated adsorption, but it appears to give the most reliable band gaps,²⁹ the direct band gap of h-BN has been experimentally estimated to be 5.97 eV,³⁰ which matches well with the value of 6.05 eV we obtained with this standard HSE06.

Following our own recommendations,¹⁷ a Martyna–Tuckerman solver³¹ was used to impose mixed boundary conditions (only periodic along the two surface directions). As reported earlier, adsorption energies on charged surfaces (or neutral materials subjected to an external electric field) are highly sensitive to periodicity normal to the surface, and lead to unreproducible errors when comparing systems with different dimensions or charge densities.¹⁷ Fundamentally, fully periodic cells will not result in realistic interaction energies. For example, according to the classical result for a charged plate, the electrostatic potential V in the vacuum region should be a linear function of the distance to the surface L , following the relation $V(L) = -\sigma L/2\epsilon_0$ (with σ being the surface charge density and ϵ_0 being the vacuum permittivity). As shown in Figure S1 (Supporting Information), this shape of the electrostatic potential is correctly obtained when the periodicity along the cell's Z direction is removed, whereas it is incorrect in the fully periodic cell. Note that besides our own report¹⁷ on the consequences of these unphysical approaches to electrostatics for chemisorption in the literature, similar observations were recently made in the context of electrochemical barriers³² and charge-driven phase transitions.³³

Absolute Versus Relative Energies in Charged Cells. We compute the adsorption energy of CO₂ on any material of charge q as

$$E_{\text{ads}}(q) = E^{\text{sheet}+\text{CO}_2}(q) - E^{\text{sheet}}(q) - E^{\text{CO}_2} \quad (1)$$

where $E^{\text{sheet}+\text{CO}_2}(q)$ is the energy of the adsorption complex at charge q , $E^{\text{sheet}}(q)$ is the energy of the nanosheet only, and E^{CO_2} is the energy of an isolated CO₂ molecule.

It is, however, not possible to directly evaluate the charging energy $E_c(q)$ of a material using a similar strategy. Electronic energies calculated in charged periodic simulation cells include an electrostatic contribution from an implicit homogenous compensating background charge: its presence is a consequence of avoiding the divergence catastrophe of charged periodic systems, and makes it impossible to directly compare energies calculated for systems of different sizes or charges. Indeed, the total energy of any charged system as obtained from periodic DFT calculations is composed of the “true” energy $E^0(q)$, and some (physically meaningless) contribution from the background charge $E^{\text{BG}}(q)$

$$E(q) = E^0(q) + E^{\text{BG}}(q) \quad (2)$$

which means that a naïve calculation of the charging energy in fact leads to

$$E(q) - E(0) = E_{\text{C}}(q) + E^{\text{BG}}(q) \quad (3)$$

with $E(q)$ being the total energy of the charged material and $E(0)$ that of the neutral system, and assuming the true charging energy should be defined as $E_{\text{C}}(q) = E^0(q) - E(0)$.

In contrast, computation of adsorption energies involves a comparison of two systems with the same cell dimensions and net charge, which means that the $E^{\text{BG}}(q)$ term is cancelled out through subtraction, a fact that is also implicitly exploited here and also in the literature. Hence, while absolute energies of charged cells are not well-defined, relative energies of cells with the same charge still carry meaning. Therefore, it should be possible to at least calculate the relative charging energy of a material, so that different materials can be compared to a common reference, as long as all charged materials have the same dimensions and charge q . Thus, one can compute a relative charging energy $E_{\text{C}}^{\text{rel}}(q)$

$$E_{\text{C}}^{\text{rel}}(q) = E(q) - E(0) - (E^{\text{ref}}(q) - E^{\text{ref}}(0)) \quad (4)$$

as long as a reference system is defined for which $E^{\text{ref}}(0)$ and $E^{\text{ref}}(q)$ can be calculated. Then, the energy terms related to the background charge will vanish, and we have

$$E_{\text{C}}^{\text{rel}}(q) = E^0(q) - E(0) - (E^{0,\text{ref}}(q) - E^{\text{ref}}(0)) \quad (5)$$

which can be used to compare charging characteristics of materials with different compositions.

In all calculations, the reference system corresponds to the pristine h-BN sheet of which the energy is evaluated at the HSE06 ($\omega = 0.11$) level.

Formation Energies of Defects. The defect formation energy at charge q can be written as

$$E_{\text{form}}^{\text{def}}(q) = E^{\text{def}}(q) - E^{\text{pristine}}(q) - \sum_i n_i \mu_i \quad (6)$$

$E^{\text{pristine}}(q)$ is the total energy of the pristine sheet (at charge q), $E^{\text{def}}(q)$ is the total energy of the defected sheet (also at charge q), μ_i is the chemical potential of the added or removed atoms, and n_i is the stoichiometry of the defect formation process. μ_i values were computed based on the total energies per atom in the reference compounds N_2 , H_2 , O_2 , and graphite for N, H, O, and C, respectively. By setting $\mu_{\text{N}} = \frac{1}{2}E_{\text{N}_2}$, we explicitly consider defect formation energies under N-rich conditions. Because the h-BN sheet is in equilibrium, the relation $\mu_{\text{BN}} = \mu_{\text{N}} + \mu_{\text{B}}$ (where μ_{BN} is the chemical potential of a single BN unit in the pristine sheet) therefore allows us to also define the value of μ_{B} under these N-rich conditions.

RESULTS AND DISCUSSION

Calculated Energetics of Charged Materials Are Highly Sensitive to the Level of Theory. As an initial test system, we consider the prototypical case¹⁰ of CO_2 adsorption on a 6×6 sheet of h-BN that carries a net charge of $2e^-$ (excess electron density of about 10^{18} m^{-2}), as shown in Figure 1a. Under these conditions, CO_2 adsorption switches from physisorption to chemisorption, for which the PBE functional²⁵ predicts a binding energy of -3.14 eV , following literature results.^{10,17}

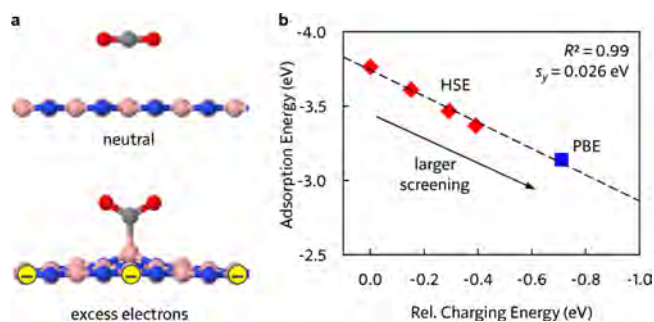


Figure 1. Charge-enhanced CO_2 adsorption at h-BN. (a) Schematic depiction of the reversible charging/adsorption process. (b) Linear scaling between the charging energy $E_{\text{C}}^{\text{rel}}(q)$ and the adsorption energy $E_{\text{ads}}(q)$ using PBE (blue square) and different flavors of HSE (red diamonds). The coefficients of determination R^2 and the standard error s_y are also shown.

A problematic aspect of the (commonly applied) PBE functional is that its accuracy and hence applicability to describe the charged material is unknown. Semilocal density functionals such as PBE are known to underestimate the band gap of materials, and can hence not necessarily be trusted for the study of processes related to electron injection. Nevertheless, all previous studies of charge-modulated chemisorption have specifically relied on calculations using PBE. Any future systematic exploration of charge-responsive material properties would therefore benefit from an assessment of the adequacy of common approximations to the exchange–correlation energy. A hybrid functional such as HSE^{26,27}—which replaces some of the PBE exchange energy term with exact (Hartree–Fock-type) exchange—performs better for band gaps and excitation energies,²⁹ but has not yet been applied to charged materials.

To gauge how the inclusion of exact exchange impacts the key properties of the charged material, we revisit the charge-induced chemisorption of CO_2 on h-BN with HSE. Specifically, we assess the impact of the effective range of the exact exchange term by using different values of the HSE screening parameter ω , in the range of 0.11–0.25 a.u. In Figure 1b, CO_2 chemisorption energies $E_{\text{ads}}(q)$ computed by these different methods are given. They are plotted as a function of the relative work of charging $E_{\text{C}}^{\text{rel}}(q)$ at the same level of theory, that is, the energy required to bring the material to charge q , relative to the absolute work of charging $E_{\text{C}}(q)$ computed at the HSE06 (i.e., $\omega = 0.11$) level. Two clear trends can be observed.

First, inclusion of exact exchange strongly increases the predicted chemisorption energy $E_{\text{ads}}(q)$, with HSE06 deviating from the PBE prediction by as much as 0.62 eV, or 20%. Such a behavior is quite unexpected: While inclusion of exact exchange is known to be a necessary requirement to avoid underestimation of the band gap²⁹—which here indeed changes from 4.65 eV (PBE) to 6.05 eV (HSE06)—chemisorption is usually already well-described at the GGA level.¹ For instance, thermochemical errors are not expected to be larger than about 0.2 eV³⁴ and CO chemisorption energies on (neutral) transition-metal surfaces as calculated by PBE and HSE06, respectively, are almost identical.³⁵

Clearly, the chemistry of charged electrocatalysts poses a hitherto unknown major challenge to common semilocal approaches to DFT. Indeed, combined with previously described convergence issues,¹⁷ previous DFT calculations for this process¹⁰ are in error by up to 1.2 eV. This is an

interesting paradox: a class of surface processes that has been almost exclusively discovered and characterized by DFT—arguably a major success story of computational materials science—also exposes as-of-yet unknown weaknesses of DFT. Future systematic explorations of these materials and processes must therefore be accompanied by a more careful and detailed investigation of the general applicability of DFT methods. In the meantime, we will henceforth use and recommend HSE06 because of its general robustness, physical transparency, and good performance for complicated electronic structures in which the self-interaction error can be important.

Second, a perfect linear correlation exists between $E_C^{\text{rel}}(q)$ and $E_{\text{ads}}(q)$. This result strongly suggests the existence of scaling laws. Not only the chemisorption energy $E_{\text{ads}}(q)$ is highly sensitive to the level of theory but also the work of charging $E_C^{\text{rel}}(q)$, which PBE underestimates by 0.71 eV, relative to HSE06. The strong correlation of these two peculiar phenomena points to a shared underlying cause which, like the band gap problem, is most likely affected by the self-interaction error in semilocal DFT. The possible existence of such a common origin of $E_C^{\text{rel}}(q)$ and $E_{\text{ads}}(q)$ also suggests that the observed linear correlation will hold in a general sense, rather than merely being an artefact of the density functional approximation.

Introduction of Defects or Impurities Can Tune Charging as Well as Adsorption Energies. Is it possible to exploit the correlation of Figure 1b in real systems, that is, systematically control the charged-state adsorption energy $E_{\text{ads}}(q)$ by tuning the charging energy $E_C(q)$ (or $E_C^{\text{rel}}(q)$) of a material? Common ways to change the electronic properties of a material are doping and defect engineering; for h-BN, various types of in-plane defects and impurities have been rather well-characterized.^{36–39} Introduction of these small imperfections in the crystal lattice does not majorly change the chemical composition of the surface; new chemistry may appear at the defect site itself, but the rest of the surface can be expected to retain its chemistry. However, such changes can dramatically change the electron affinity of the material, and thus allows for a controlled exploration specifically of the impact of charging properties on the surface chemistry. Furthermore, the effect of defects on charge-responsive adsorption chemistry has not yet been systematically studied.⁸

We consider two types of vacancy defects (boron vacancy V_B and nitrogen vacancy V_N), substitution of N by B (B_N) and vice versa (N_B), two types of substitutions by C (C_N and C_B), the most common substitution by O (O_N), and a H-passivated V_B defect ($V_B\text{-3H}$). Of these simple in-plane defects, C_B , O_N , and $V_B\text{-3H}$ were found to be very common in h-BN samples.³⁸ Each material model contains a single defect, the charging energy $E_C^{\text{rel}}(q)$ —with $q = 2e^-$ —is computed at the HSE06 level relative to pristine h-BN, and the CO_2 adsorption energy $E_{\text{ads}}(q)$ is calculated for adsorption sites away from the defect. If possible, we also calculate the adsorption energy at the defect site, which is labeled $E_{\text{ads}}^{\text{def}}(q)$. All these values are summarized in Table 1.

In almost all cases, in-plane defects reduce the work of charging (i.e., more negative) and, consequently, decrease the chemisorption strength (i.e., closer to zero). This effect is even so large for V_B , B_N , and C_N that no chemisorption is found to take place at all. When plotted in Figure 2, a striking linear correlation between $E_C^{\text{rel}}(q)$ and $E_{\text{ads}}(q)$ can be observed, in keeping with our earlier observation on pristine h-BN. That is, a linear correlation for $E_{\text{ads}}(q) < 0$ only, once $E_C^{\text{rel}}(q)$ becomes

Table 1. Relative Charging Energies $E_C^{\text{rel}}(q)$ and Adsorption Energies $E_{\text{ads}}(q)$ and $E_{\text{ads}}^{\text{def}}(q)$ for CO_2 at Different (Defected) Types of Charged h-BN^a

	$E_C^{\text{rel}}(q)$	$E_{\text{ads}}(q)^b$	$E_{\text{ads}}^{\text{def}}(q)$
pristine	0.00	−3.76	n/a
V_B	−6.95	n/a	−1.49
V_N	−2.55	−1.36	−3.87
B_N	−4.72	n/a	−1.75
N_B	−2.65	−1.21	−2.42
C_N	−3.93	n/a	−0.58
C_B	−1.25	−2.55	−2.92
O_N	−0.86	−3.26	−4.06
$V_B\text{-3H}$	0.02	−3.72	n/a

^aAll Energies in eV. ^bOnly chemisorption energies are considered. Physisorption or nonexistent configurations are indicated as n/a.

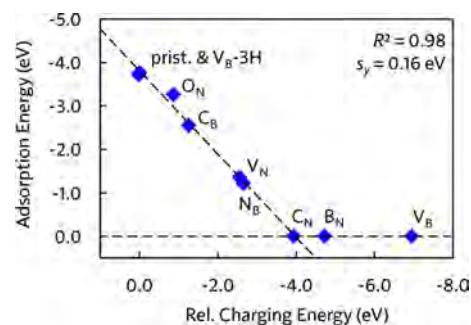


Figure 2. Correlation between the charging energy $E_C^{\text{rel}}(q)$ and the adsorption energy on the crystalline sites on the nanosheet, $E_{\text{ads}}(q)$.

low enough, no chemisorption is possible anymore. The fitted relation $E_{\text{ads}}(q) = a + bE_C^{\text{rel}}(q)$ has $a = -3.81$ eV and $b = -0.96$ for this particular surface dimension and charge. According to these fitted values, $E_C^{\text{rel}}(q) \approx -4$ eV coincides with a crossover between chemi- and physisorption, consistent with our observations.

Interestingly, the fitted linear parameters for the different defect systems retroactively confirm the generality of the tentative conclusions drawn from the comparison of different density functional approximations (Figure 1b). For that set of calculations, we obtain $a = -3.74$ eV and $b = -0.88$. Given that estimated uncertainties on the slopes are in the order of 0.05, the fitted relation appears to be universal for h-BN and its derivatives, regardless of how the charging energy is tuned.

For the particular adsorption mode considered, the only difference between materials is the presence of remote defects; the actual bonding pattern between CO_2 and the surface remains the same and a very “clean” comparison becomes possible. To investigate to what extent our newly discovered linear scaling relation holds for different surface chemistries, we also compared $E_{\text{ads}}^{\text{def}}(q)$ values. Here, we can distinguish between different bonding patterns involving B– CO_2 , N– CO_2 , and C– CO_2 single bonds, and also more complex coordinations with vacancy defects (Figure 3a–c, and Supporting Information). Yet, even within these tremendous variations in surface chemistry, linear scaling relations can still be observed (Figure 3d). However, sizable deviations from the linear regime remain. This is partly because the value of $E_{\text{ads}}^{\text{def}}(q)$ in some cases contains contributions other than pure charge-enhancement effects. Indeed, CO_2 can already chemisorb on some defects even at neutral charge, that is, $E_{\text{ads}}^{\text{def}}(0) < 0$, in contrast to pristine h-BN or nondefect sites, where all

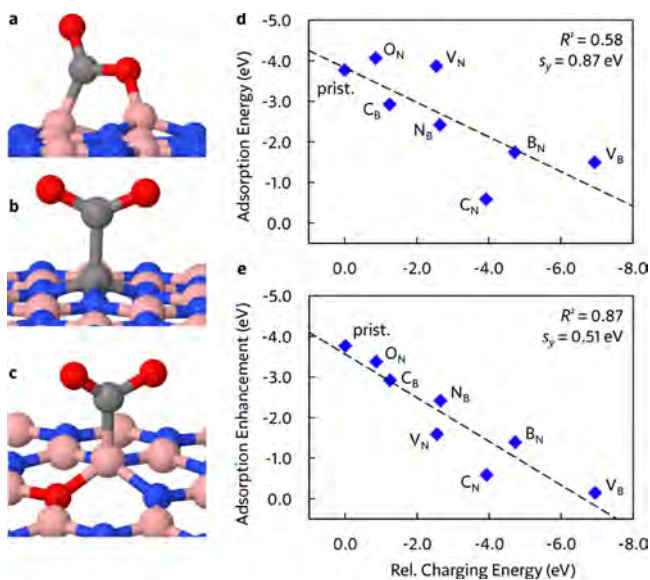


Figure 3. Adsorption at defect sites. Example adsorption configurations at (a) V_N, (b) C_B, and (c) O_N. (d) Correlation between the adsorption energy $E_{\text{ads}}^{\text{def}}(q)$ and relative charging energy $E_{\text{C}}^{\text{rel}}(q)$. (e) Correlation between the adsorption enhancement due to charging $E_{\text{ads}}^{\text{def}}(0 \rightarrow q)$ and $E_{\text{C}}^{\text{rel}}(q)$.

chemisorption is solely attributable to charging effects. This is the case for the two vacancies ($E_{\text{ads}}^{\text{def}}(0)$) of -1.35 eV for V_B and -2.28 eV for V_N) and also B_N (-0.36 eV) and O_N (-0.69 eV). In order to separate neutral-state surface chemistry (i.e., intrinsic chemical properties of the neutral material) from charge-induced properties, we can define the adsorption enhancement due to charging

$$E_{\text{ads}}^{\text{def}}(0 \rightarrow q) = E_{\text{ads}}^{\text{def}}(q) - E_{\text{ads}}^{\text{def}}(0) \quad (7)$$

When plotting $E_{\text{ads}}^{\text{def}}(0 \rightarrow q)$ versus $E_{\text{C}}^{\text{rel}}(q)$ in Figure 3e, a much clearer linear correlation is observed. Here, the fitted intercept and slope are $a = -3.56$ eV and $b = -0.54$, respectively. This suggests that charging effects can even be described by linear scaling relations across different surface chemistries and bonding patterns, provided that only specific charge-related additive contributions are considered.

Correlation between Work of Charging and Chemisorption: Physical Interpretation. The linear coefficients of the observed correlations can be given a physical meaning as well. First, the x -intercept ($E_{\text{C}}^{\text{rel}}(q) = -a/b$, where $E_{\text{ads}}^{\text{def}}(0 \rightarrow q) = 0$) defines the lowest work of charging required to induce any stimulation of chemisorption. It can be thought of as a threshold charging energy of sorts. On one hand, adsorption at defect sites is comparatively easier to stimulate, as effects can already be observed when $E_{\text{C}}^{\text{rel}}(q) > -6.6$ eV, while adsorption at crystalline h-BN sites needs $E_{\text{C}}^{\text{rel}}(q) > -4.0$ eV. On the other hand, the slope b is a measure of the efficiency by which the work of charging is transferred to adsorption stimulation, that is, its absolute value is the fraction of the work of charging that is recovered as chemisorption energy. Once past the threshold charging energy, adsorption is stimulated much more efficiently at crystalline sites: $|b| \approx 1$, so almost all of the additionally supplied work of charging directly stimulates adsorption, while about half of that energy is lost if adsorption occurs at defect sites.

From these linear relations, some general principles can be deduced. The cost to charge a particular material can be

reduced through strategic doping which, however, also reduces the binding strength on the surface sites of interest. Moreover, different chemical (or possibly structural) surface features on a charged material exhibit a different efficiency by which they convert the work of charging into enhancement of the adsorption process. As such, the value of our observed correlations becomes clear, linear scaling relations connect the properties of different material compositions, offering a simple roadmap toward the discovery and optimization of new materials with particular electrocatalytic properties. It must be mentioned that there appears to be some evidence that our conclusions will hold among a wider range of materials: easy-to-charge narrow-gap materials generally exhibit weaker charge-enhance binding than wide-gap materials, or need larger charge densities to achieve similar binding.⁸ However, a direct comparison across literature studies is not possible due to inconsistencies in many computational setups.¹⁷ Differences in the relative charging energy can be experimentally probed by measuring the required applied potential in an electrostatic gating procedure to achieve a certain charge state.¹²

We note that, strictly speaking, our analysis only applies at fixed charge density. However, it has been suggested that the work of charging and the charge density are linearly correlated as well,⁸ which implies that our conclusions will hold for energies of charging to arbitrary densities. Of course, any previously reported correlations between charge densities, work of charging, or adsorption energies were strictly within a single system; here, we have shown how such relations extend across different materials. Experiments have also pointed to the existence of electron-induced surface chemistry.⁴⁰

Excess Electrons Stabilize Most Defects. The formation energies for the defects discussed in the manuscript are collected in Table 2 for neutral sheets. These values closely

Table 2. Defect Formation Energies $E_{\text{form}}^{\text{def}}$ in Neutral ($E_{\text{form}}^{\text{def}}(0)$) and Charged ($E_{\text{form}}^{\text{def}}(q)$) h-BN Sheets^{a,b}

	$E_{\text{C}}^{\text{rel}}(q)$	$E_{\text{form}}^{\text{def}}(0)$	$E_{\text{form}}^{\text{def}}(q)$
V _B	-6.95	7.45	0.50
V _N	-2.55	8.38	5.83
B _N	-4.72	9.40	4.68
N _B	-2.65	4.35	1.70
C _N	-3.93	4.10	0.17
C _B	-1.25	1.83	0.58
O _N	-0.86	1.62	0.76
V _B -3H	0.02	-0.20	-0.18

^aRelative charging energies of the defects systems are also reported for convenience of the reader. ^bAll energies in eV.

match those reported by Huang & Lee for V_B (7.65 eV), V_N (8.47 eV), C_N (~ 4.4 eV), and C_B (1.76 eV) under the same (N-rich) conditions, which were also calculated with HSE06.³⁷

We note that the value of $E_{\text{C}}^{\text{rel}}(q)$ for defect systems has an additional physical meaning; it also corresponds to the change in defect formation energy upon charging. Indeed, the change in defect formation energy due to charging can be written as follows

$$\begin{aligned} E_{\text{form}}^{\text{def}}(q) - E_{\text{form}}^{\text{def}}(0) \\ = (E^{\text{def}}(q) - E^{\text{pristine}}(q)) - (E^{\text{def}}(0) - E^{\text{pristine}}(0)) \end{aligned} \quad (8)$$

Because the relative charging energy for each system is defined relative to that of the pristine h-BN sheet, we also have the following expression for the relative charging energy of the defect system

$$E_C^{\text{rel,def}}(q) = E^{\text{def}}(q) - E^{\text{def}}(0) - (E^{\text{pristine}}(q) - E^{\text{pristine}}(0)) \quad (9)$$

and combination of the two expressions leads to

$$E_{\text{form}}^{\text{def}}(q) - E_{\text{form}}^{\text{def}}(0) = E_C^{\text{rel,def}}(q) \quad (10)$$

Therefore, the relative charging energy of a doped or defected sheet is equal to the absolute (de)stabilization of said defect upon charging.

Because $E_C^{\text{rel}}(q) < 0$ in most considered cases, it can be inferred that negative charging promotes the formation of these point defects, which can also be seen by comparing $E_{\text{form}}^{\text{def}}(0)$, $E_{\text{form}}^{\text{def}}(q)$, and $E_C^{\text{rel,def}}(q)$ in Table 2. A reversal in relative stabilities of the defects is induced upon charging. While C_B , O_N , and $V_B\text{-}3H$ are the most stable in the neutral sheet, charging results in V_B , C_N , and $V_B\text{-}3H$ becoming the most favorable defects, all with formation energies below 0.5 eV. While only for $V_B\text{-}3H$ we find $E_{\text{form}}^{\text{def}} < 1.0$ eV at zero charge, this is already the case for six of the defects upon charging. This fact could perhaps be exploited to stimulate the synthesis of specific defects. Evidently, these conclusions are quantitatively valid only for the specific charge states and system sizes considered here.

CONCLUSIONS

We here report the first ever linear scaling relation for charge-modulated gas adsorption on 2D nanomaterials. Electron injection is associated with a material-specific charging energy $E_C(q)$, which is linearly correlated with the CO_2 adsorption energy $E_{\text{ads}}(q)$ on the charged material. A generalized form of the scaling relation—between $E_C(q)$ and the adsorption enhancement due to charging $E_{\text{ads}}(0 \rightarrow q)$ —also holds across different materials and bonding patterns. These relations describe the threshold charging energy required to observe charge-stimulated adsorption in a class of materials, and the efficiency by which additional work of charging is converted into improved chemisorption beyond this point. $E_C(q)$ of a given material can be effectively controlled by doping or defect engineering and is a new vector along which surface chemistry can be tuned, allowing to identify or design materials with specific charge-response properties.

Moreover, we find that the predicted value of $E_C(q)$, and consequently $E_{\text{ads}}(q)$, is very sensitive to the applied DFT functional; previous investigations of charge-modulated adsorption have relied on semilocal DFT, and therefore might have reported energies in error by up to 1 eV relative to hybrid DFT. Besides their technological potential, charged nanomaterials are therefore also an intriguing challenge for computational materials science, and will likely be a useful test case for new quantum chemical approaches. However, the relative performance of different model chemistries are a manifestation of deeper principles and can hence also reveal phenomena of actual physical relevance, as demonstrated here.

These results further confirm that charge-switchable surface chemistry is a powerful technology which can play an important role in environmental applications such as gas capture, storage, and conversion. The fundamental principles

unraveled in this work will help lead the way to applications as well as have an impact on theory.

ASSOCIATED CONTENT

Supporting Information

The Supporting Information is available free of charge on the ACS Publications website at DOI: 10.1021/acs.jpcc.9b01216.

Dependence of the vacuum electrostatic potential on the use of periodic boundary conditions and graphical representations of different adsorption complexes along with their key geometric parameters (PDF)

AUTHOR INFORMATION

Corresponding Author

*E-mail: kristof.bal@uantwerpen.be.

ORCID

Kristof M. Bal: 0000-0003-2467-1223

Erik C. Neyts: 0000-0002-3360-3196

Notes

The authors declare no competing financial interest.

ACKNOWLEDGMENTS

K.M.B. was funded as PhD fellow (aspirant) of the FWO-Flanders (Research Foundation—Flanders), Grant 11V8915N. The computational resources and services used in this work were provided by the VSC (Flemish Supercomputer Center), funded by the FWO and the Flemish Government—department EWI.

REFERENCES

- Greeley, J. Theoretical Heterogeneous Catalysis: Scaling Relationships and Computational Catalyst Design. *Annu. Rev. Chem. Biomol. Eng.* **2016**, *7*, 605–635.
- Logadottir, A.; Rod, T. H.; Nørskov, J. K.; Hammer, B.; Dahl, S.; Jacobsen, C. J. H. The Brønsted–Evans–Polanyi Relation and the Volcano Plot for Ammonia Synthesis over Transition Metal Catalysts. *J. Catal.* **2001**, *197*, 229–231.
- Nørskov, J. K.; Bligaard, T.; Logadottir, A.; Bahn, S.; Hansen, L. B.; Bollinger, M.; Bengaard, H.; Hammer, B.; Slijvančanin, Z.; Mavrikakis, M.; et al. Universality in Heterogeneous Catalysis. *J. Catal.* **2002**, *209*, 275–278.
- Kakekhani, A.; Ismail-Beigi, S. Ferroelectric-Based Catalysis: Switchable Surface Chemistry. *ACS Catal.* **2015**, *5*, 4537–4545.
- Che, F.; Gray, J. T.; Ha, S.; McEwen, J.-S. Improving Ni Catalysts Using Electric Fields: A DFT and Experimental Study of the Methane Steam Reforming Reaction. *ACS Catal.* **2017**, *7*, 551–562.
- Bal, K. M.; Huygh, S.; Bogaerts, A.; Neyts, E. C. Effect of Plasma-Induced Surface Charging on Catalytic Processes: Application to CO_2 Activation. *Plasma Sources Sci. Technol.* **2018**, *27*, 024001.
- Mehta, P.; Barboun, P.; Herrera, F. A.; Kim, J.; Rumbach, P.; Go, D. B.; Hicks, J. C.; Schneider, W. F. Overcoming Ammonia Synthesis Scaling Relations with Plasma-Enabled Catalysis. *Nat. Catal.* **2018**, *1*, 269–275.
- Tan, X.; Tahini, H. A.; Smith, S. C. Computational Design of Two-Dimensional Nanomaterials for Charge Modulated CO_2/H_2 Capture and/or Storage. *Energy Storage Mater.* **2017**, *8*, 169–183.
- Zhou, J.; Wang, Q.; Sun, Q.; Jena, P.; Chen, X. S. Electric Field Enhanced Hydrogen Storage on Polarizable Materials Substrates. *Proc. Natl. Acad. Sci. U.S.A.* **2010**, *107*, 2801–2806.
- Sun, Q.; Li, Z.; Searles, D. J.; Chen, Y.; Lu, G.; Du, A. Charge-Controlled Switchable CO_2 Capture on Boron Nitride Nanomaterials. *J. Am. Chem. Soc.* **2013**, *135*, 8246–8253.

- (11) Qin, G.; Du, A.; Sun, Q. A Theoretical Insight into a Feasible Strategy for the Fabrication of Borophane. *Phys. Chem. Chem. Phys.* **2018**, *20*, 16216–16221.
- (12) Wang, Y.; Xiao, J.; Zhu, H.; Li, Y.; Alsaid, Y.; Fong, K. Y.; Zhou, Y.; Wang, S.; Shi, W.; Wang, Y.; et al. Structural Phase Transition in Monolayer MoTe₂ Driven by Electrostatic Doping. *Nature* **2017**, *550*, 487–491.
- (13) Tan, X.; Kou, L.; Tahini, H. A.; Smith, S. C. Conductive Graphitic Carbon Nitride as an Ideal Material for Electrocatalytically Switchable CO₂ Capture. *Sci. Rep.* **2015**, *5*, 17636.
- (14) Qin, G.-Q.; Du, A.-J.; Sun, Q. Charge- and Electric-Field-Controlled Switchable Carbon Dioxide Capture and Gas Separation on a C₂N Monolayer. *Energy Technol.* **2018**, *6*, 205–212.
- (15) Li, X.; Guo, T.; Zhu, L.; Ling, C.; Xue, Q.; Xing, W. Charge-Modulated CO₂ Capture of C₃N Nanosheet: Insights from DFT Calculations. *Chem. Eng. J.* **2018**, *338*, 92–98.
- (16) Tan, X.; Tahini, H. A.; Smith, S. C. Borophene as a Promising Material for Charge-Modulated Switchable CO₂ Capture. *ACS Appl. Mater. Interfaces* **2017**, *9*, 19825–19830.
- (17) Bal, K. M.; Neyts, E. C. Modelling Molecular Adsorption on Charged or Polarized Surfaces: A Critical Flaw in Common Approaches. *Phys. Chem. Chem. Phys.* **2018**, *20*, 8456–8459.
- (18) VandeVondele, J.; Krack, M.; Mohamed, F.; Parrinello, M.; Chassaing, T.; Hutter, J. Quickstep: Fast and Accurate Density Functional Calculations Using a Mixed Gaussian and Plane Waves Approach. *Comput. Phys. Commun.* **2005**, *167*, 103–128.
- (19) Hutter, J.; Iannuzzi, M.; Schiffrmann, F.; VandeVondele, J. CP2K: Atomistic Simulations of Condensed Matter Systems. *Wiley Interdiscip. Rev.: Comput. Mol. Sci.* **2014**, *4*, 15–25.
- (20) Lippert, G.; Hutter, J.; Parrinello, M. A Hybrid Gaussian and Plane Wave Density Functional Scheme. *Mol. Phys.* **1997**, *92*, 477–488.
- (21) Goedecker, S.; Teter, M.; Hutter, J. Separable Dual-Space Gaussian Pseudopotentials. *Phys. Rev. B: Condens. Matter Mater. Phys.* **1996**, *54*, 1703–1710.
- (22) Krack, M. Pseudopotentials for H to Kr Optimized for Gradient-Corrected Exchange-Correlation Functionals. *Theor. Chem. Acc.* **2005**, *114*, 145–152.
- (23) VandeVondele, J.; Hutter, J. Gaussian Basis Sets for Accurate Calculations on Molecular Systems in Gas and Condensed Phases. *J. Chem. Phys.* **2007**, *127*, 114105.
- (24) Guidon, M.; Hutter, J.; VandeVondele, J. Auxiliary Density Matrix Methods for Hartree–Fock Exchange Calculations. *J. Chem. Theory Comput.* **2010**, *6*, 2348–2364.
- (25) Perdew, J. P.; Burke, K.; Ernzerhof, M. Generalized Gradient Approximation Made Simple. *Phys. Rev. Lett.* **1996**, *77*, 3865–3868.
- (26) Heyd, J.; Scuseria, G. E.; Ernzerhof, M. Hybrid Functionals Based on a Screened Coulomb Potential. *J. Chem. Phys.* **2003**, *118*, 8207–8215.
- (27) Krukau, A. V.; Vydrov, O. A.; Izmaylov, A. F.; Scuseria, G. E. Influence of the Exchange Screening Parameter on the Performance of Screened Hybrid Functionals. *J. Chem. Phys.* **2006**, *125*, 224106.
- (28) Perdew, J. P.; Ernzerhof, M.; Burke, K. Rationale for Mixing Exact Exchange with Density Functional Approximations. *J. Chem. Phys.* **1996**, *105*, 9982–9985.
- (29) Garza, A. J.; Scuseria, G. E. Predicting Band Gaps with Hybrid Density Functionals. *J. Phys. Chem. Lett.* **2016**, *7*, 4165–4170.
- (30) Watanabe, K.; Taniguchi, T.; Kanda, H. Direct-Bandgap Properties and Evidence for Ultraviolet Lasing of Hexagonal Boron Nitride Single Crystal. *Nat. Mater.* **2004**, *3*, 404–409.
- (31) Martyna, G. J.; Tuckerman, M. E. A Reciprocal Space Based Method for Treating Long Range Interactions in Ab Initio and Force-Field-Based Calculations in Clusters. *J. Chem. Phys.* **1999**, *110*, 2810–2821.
- (32) Van den Bossche, M.; Skúlason, E.; Rose-Petruck, C.; Jónsson, H. Assessment of Constant-Potential Implicit Solvation Calculations of Electrochemical Energy Barriers for H₂ Evolution on Pt. *J. Phys. Chem. C* **2019**, *123*, 4116–4124.
- (33) Patil, U.; Caffrey, N. M. Composition Dependence of the Charge Driven Phase Transition in Group-VI Transition Metal Dichalcogenides. **2019**, arXiv preprint arXiv:1901.02697.
- (34) Goerigk, L.; Hansen, A.; Bauer, C.; Ehrlich, S.; Najibi, A.; Grimme, S. A Look at the Density Functional Theory Zoo with the Advanced GMTKN55 Database for General Main Group Thermochemistry, Kinetics and Noncovalent Interactions. *Phys. Chem. Chem. Phys.* **2017**, *19*, 32184–32215.
- (35) Stroppa, A.; Kresse, G. The Shortcomings of Semi-Local and Hybrid Functionals: What We Can Learn from Surface Science Studies. *New J. Phys.* **2008**, *10*, 063020.
- (36) Azevedo, S.; Kaschny, J. R.; de Castilho, C. M. C.; de Brito Mota, F. Theoretical Investigation of Defects in a Boron Nitride Monolayer. *Nanotechnology* **2007**, *18*, 495707.
- (37) Huang, B.; Lee, H. Defect and Impurity Properties of Hexagonal Boron Nitride: A First-Principles Calculation. *Phys. Rev. B: Condens. Matter Mater. Phys.* **2012**, *86*, 245406.
- (38) McDougall, N. L.; Partridge, J. G.; Nicholls, R. J.; Russo, S. P. D.; McCulloch, G. Influence of Point Defects on the Near Edge Structure of Hexagonal Boron Nitride. *Phys. Rev. B: Condens. Matter Mater. Phys.* **2017**, *96*, 144106.
- (39) Weston, L.; Wickramaratne, D.; Mackoite, M.; Alkauskas, A.; Van de Walle, C. G. Native Point Defects and Impurities in Hexagonal Boron Nitride. *Phys. Rev. B: Condens. Matter Mater. Phys.* **2018**, *97*, 214104.
- (40) Lee, J.; Sorescu, D. C.; Deng, X. Electron-Induced Dissociation of CO₂ on TiO₂(110). *J. Am. Chem. Soc.* **2011**, *133*, 10066–10069.